Incoherent Scattering of Light from Anisotropic Degenerate Plasmas

P. M. PLATZMAN
Bell Telephone Laboratories, Murray Hill, New Jersey
(Received 17 February 1965)

The differential scattering cross section for monochromatic radiation incident on an anisotropic degenerate plasma is calculated. The charge carriers are assumed to have ellipsoidal energy surfaces such that relatively undamped plasma acoustic modes exist. The line shape of the scattered radiation depends strongly on the existence of degeneracy and on the nature of the anisotropy. The scattering for small values of energy (ω) and momentum (q) transferred to the plasma is dominated by the excitation of plasma acoustic modes. The spectrum of the scattered radiation exhibits a dip for values of $\omega/q=V_F$. Numerical calculations of the differential scattering cross section for a typical set of parameters are presented. The effects of an externally imposed electron drift are included.

I. INTRODUCTION

IT is well known that inelastic scattering of electromagnetic radiation from a plasma can provide useful information about the excitation spectrum of the medium. If the material is almost transparent to the radiation, the differential scattering cross section as a function of momentum (q) and energy transfer (ω) is a direct measure of the density-density correlation function for the system.[1] When the momentum transfer to the system corresponds to wavelengths which are large compared with typical screening lengths (λ_S) in the plasma, the line shape of the scattered radiation depends on the collective excitations of the plasma. In the opposite limit, when the momentum-transfer wavelengths are short compared to typical screening lengths, the single-particle excitation spectrum is reflected in the line shape of the scattered radiation.

Typical screening lengths (Debye screening for a nondegenerate plasma, Fermi-Thomas screening for a degenerate plasma) vary over a wide range. For an ionospheric plasma with a density $n\approx10^5$ cm^{-3} and a temperature $kT\approx0.1$ eV, the Debye length ($\lambda_S\equiv\lambda_D\equiv q_D^{-1}$) is of the order of 100 cm. For a laboratory discharge with density $n\approx10^{12}-10^{16}$ cm^{-3}, and for temperature $kT\approx10$ eV, the Debye length is $\lambda_D\sim10^{-2}-10^{-4}$ cm. For a degenerate semiconducting plasma with a Fermi energy of 30 meV (millielectron volts) and an effective mass of a few tenths of a free-electron mass the Fermi-Thomas screening length is of the order of $(\lambda_S\equiv\lambda_{FT}\equiv q_{FT}^{-1})10^{-7}$ cm.

Experiments using high-power radar beams in the megacycle range have been carried out in the ionosphere.[2] Since the wavelength of the electromagnetic (E.M.) radiation is considerably larger than the Debye length for the plasma, the scattering was from the "collective" modes. Recently, there have been a number of experiments reported on the scattering of laser light ($\hbar\omega\approx1$ eV) from laboratory discharges. The wavelength of the laser light at 1 eV is approximately 10^{-4} cm, i.e., of the order of (in general somewhat smaller than) the typical Debye lengths. By changing the angle of scattering it should be possible to see both collective and single-particle oscillations in these laboratory plasmas. To date, most of the experiments which have been reported are all in the single-particle high-momentum transfer regime, although there have been a few preliminary experiments reported which do exhibit collective effects.[3] The laser is apparently an ideal tool for studying the incoherent scattering of light from laboratory plasmas. Its wavelength is in the correct region and its narrow spectral width should enable one to resolve the relatively small shifts in energy which are associated with the incoherent scattering, typically of the order of 1 part in 10^4.

There have appeared many theoretical analyses[1,4,5] of the scattering of light from nondegenerate isotropic classical plasmas. The purpose of the present paper is to analyze the scattering of laser light in the region around 1 eV from degenerate semiconducting plasmas (i.e., the electrons in the conduction band of a doped semiconductor). We will take into account within the framework of a simple ellipsoidal model both the degeneracy and mass anisotropy of such plasmas.

It is reasonable to take for typical semiconducting plasmas the long-wavelength collective limit (see earlier discussion). In order to qualitatively understand the kind of scattering cross section we will obtain in a more detailed analysis let us consider the case of an isotropic degenerate plasma. The many-valleyed anisotropic semiconducting plasma will behave like a multiple-component isotropic plasma. In our simple model the anisotropy will in effect introduce a spread of mass values for the carriers.

[1] E. E. Salpeter, Phys. Rev. **120**, 1528 (1960).
[2] K. W. Bowlers, Phys. Rev. Letters **1**, 454 (1958); V. C. Pineo, L. G. Craft, and H. W. Briscol, J. Geophys. Res. **65**, 2629 (1960).
[3] S. A. Ramsden and W. E. R. Davies, Phys. Rev. Letters **13**, 277 (1964); G. Fiocco and E. Thompson, *ibid.* **10**, 89 (1963); L. A. Farrow and S. J. Buchsbaum, Bull. Am. Phys. Soc. **10**, No. 2, 226 (1965); E. Gerry, *ibid.* 226 (1965); D. R. Sigman, J. F. Holt, and M. L. Pool, *ibid.* 226 (1965); R. M. Patrick and E. T. Gerry, *ibid.* 226 (1965).
[4] J. P. Dougherty and D. T. Farley, Proc. Roy. Soc. (London) **A259**, 79 (1960); A. Ron, J. Dawson, and C. Oberman, Phys. Rev. **132**, 479 (1963); D. C. Dubois and V. Gilinski, *ibid.* **133**, A1308 (1964), hereafter referred to as D.G.
[5] M. N. Rosenbluth and N. Rostoker, Phys. Fluids **5**, 776 (1962).

In the long-wavelength region (for an isotropic system) the spectrum and magnitude of the scattering cross section depends critically on the number of species of charge carriers in the plasma. For a single-component plasma (at long wavelengths) the scattered radiation lies almost entirely in the so-called plasma line. This simply means that the monochromatic incident frequency is shifted by a fixed amount $\omega_p=(4\pi ne^2/m^*\epsilon_0)^{1/2}$, and broadened into a Lorentzian by short-range collisional effects. The cross-sectional area under this line is of order $\sigma_{\text{plasmon}}\approx(q/q_{\text{FT}})^2r_0^2$, where $r_0=e^2/mc^2$ is the classical radius of the electron. All cross sections are normalized per particle per unit volume per unit solid angle. The area under the free-particle-like Doppler-broadened Thompson scattering which occurs for much smaller values of the frequency shift ($\omega/qV_F\approx1$ where V_F is the Fermi velocity) is smaller than that under the plasma line by a factor $(q/q_{\text{FT}})^2$. The reason that almost all of the scattering cross section is in the plasma line results from the fact that plasma oscillations at frequencies $\omega\sim\omega_p$ are the only longitudinal collective modes for a one-component plasma.

For a two-component isotropic plasma the differential scattering cross section is completely changed. There are now two types of collective longitudinal oscillations. There is a plasma oscillation-like mode having a frequency which is approximately given by the density and mass of the lighter carrier. There is also a sound-like mode with $\omega=qV_S$, where V_S is the sound velocity and is of the order of (somewhat larger than) the characteristic velocities (thermal, or Fermi) of the heavy carriers. Dynamically the sound modes comes from a static screening of the heavy carriers by the light ones. The force between heavy carriers then is effectively short-range (no longer $1/r$, but like $\exp(-q_{\text{FT}}r)/r$) and long-wavelength density fluctuations can be excited with only a small expenditure of energy. The plasma oscillations require a finite energy (frequency) to excite even at infinitely long wavelengths.

In the differential scattering cross section, the sound modes show up as a line (possibly broad) for small values of the frequency shift $\omega\approx qV_S$ where $\omega\ll\omega_p$. This is the so-called central line. The area under this central line is easily shown to be of order r_0^2, i.e., large compared to the area under the plasma line. It has been shown[5] for a nondegenerate plasma, that when the temperatures of the two species are equal the acoustic mode has a short lifetime and is not well defined. In this case the acoustic mode will not show up as a sharp peak in the "central line." For a degenerate anisotropic plasma, on the other hand, this conclusion is no longer valid. In fact, for reasonably small values of the anisotropy ratio (mass ratio) we will show that there is a well-defined acoustic mode and that these acoustic modes in the long-wavelength limit dominate the scattering from this kind of a degenerate plasma.

In Sec. II we present the model and formally calculate the differential scattering cross section for light for an arbitrary number of ellipsoidal carriers. The formula is evaluated within the framework of the random-phase or self-consistent field approximation. In Sec. III the differential scattering cross section for a single ellipsoidal carrier is discussed in some detail. In Sec. IV we give a discussion of the scattering cross section for two ellipsoidal carriers. The effect of carrier drift on the scattering cross section is also discussed. In Sec. V we present a numerical calculation of the differential scattering cross section for the two-ellipsoid case. We also discuss the kinds of experimental parameters one should have in order to observe this scattering.

II. THE MODEL

For the purpose of this paper we will assume that the "plasma" is made up of a set of (N) separate ellipsoids of revolution. The Hamiltonian that describes such a system is

$$H=\frac{1}{2m}\sum_{l=1}^{N}\int d^3x\Psi_l^\dagger(x)[-\nabla_i\nabla_j\mu_{ij}^{(l)}\Psi_l(x)]+\frac{e^2}{2}\int d^3xd^3x'\rho(x)\frac{1}{|\mathbf{x}-\mathbf{x}'|}\rho(x'), \quad (1)$$

where

$$\rho(x)=\sum_{l=1}^{N}\Psi_l^\dagger(x)\Psi_l(x). \quad (2)$$

The operators $\Psi_l(x)$ are the usual second-quantized field operators for the lth particle and $\mu_{ij}^{(l)}$ are the effective inverse mass tensors for the charge carriers measured in terms of the free-electron mass m. The effect of the periodic lattice is retained only insofar as it manifests itself in the effective mass tensor $\mu_{ij}^{(l)}$. For energy and momentum transfers small compared to interband energies and reciprocal lattice vectors respectively, there will always exist an effective one-band Hamiltonian of the form given in Eq. (1).[6] The energy-momentum relation of the particles will not necessarily be quadratic. However, a quadratic anisotropic energy surface is a reasonably good model for the conduction band of some lightly doped semiconductors.[7] In addition, the ellipsoidal model will, in a concrete manner, incorporate the essential features of anisotropy into the differential scattering cross section.

The coupling to the electromagnetic field is obtained by replacing ∇_i by (∇_i-e/cA_i) in the usual way. It has been shown (see D. G. and Ref. 8) that for a wide range of parameters, namely, $E_f\ll\hbar\omega_e\ll mc^2$ (where ω_e is the external frequency of the light, E_f the Fermi energy, and m a typical mass of one of the carriers) that one can

[6] E. I. Blount, in *Solid State Physics*, edited by F. Seitz and D. Turnbull (Academic Press Inc., New York, 1962), Vol. 13, p. 305.

[7] T. H. Geballe, in *Semiconductors*, edited by N. B. Hannay (Reinhold Publishing Company, New York, 1960), p. 320.

[8] P. M. Platzman and N. Tzoar, Phys. Rev. **136**, A11 (1964).

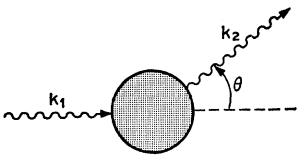

FIG. 1. Diagrammatical representation of the incoherent scattering process. The shaded region is the plasma; the wiggly lines represent the photons.

drop the terms linear in the vector potential and consider only the coupling of the incoming and outgoing radiation via the $e^2A_iA_j\mu_{ij}{}^{(l)}/2mc^2$ in the Hamiltonian. This essentially nonrelativistic approximation leads in a straightforward way to the following expression for the differential scattering cross section for a photon of wave vector $\mathbf{k}_1$, frequency ω_1, and polarization $\mathbf{e}_1$ to be scattered into a state with wave vector $\mathbf{k}_2$, frequency ω_2, and polarization $\mathbf{e}_2$ (see Fig. 1):

$$\frac{d\sigma}{d\omega d\Omega}=\frac{r_0^2}{(2\pi)}\frac{1}{(1-e^{-\beta\omega})}\left(\frac{\omega_2}{\omega_1}\right)\times\mathrm{Re}\left[\int_0^\infty dt e^{i\omega t}\langle[\hat{\rho}_q(t),\hat{\rho}_{-q}(0)]\rangle\right], \quad (3)$$

where

$$\omega=\omega_1-\omega_2,$$
$$\mathbf{q}=\mathbf{k}_1-\mathbf{k}_2,$$
$$\beta=1/k_BT,$$

and

$$r_0=e^2/m$$

is the classical electron radius. We will use units in which $\hbar=c=1$.

The angular bracket means the usual thermal ensemble average, i.e.,

$$\langle O\rangle=\mathrm{Tr}\{e^{\beta(\Omega+\mu N-H)}O\} \quad (4)$$

and the square bracket inside the average is the commutator of $\hat{\rho}_q(t)$ and $\hat{\rho}_{-q}(0)$. The operator $\hat{\rho}_{-q}(0)$ is a slightly modified (modified to include polarization factor) density operator, i.e.,

$$\hat{\rho}_q(0)=\sum_{l=1}^N\int\Psi_l{}^\dagger(\mathbf{x})\Psi_l(\mathbf{x})\alpha^l e^{i\mathbf{q}\cdot\mathbf{x}}d^3q, \quad (5)$$

where

$$\alpha^l=\mathbf{e}_1\cdot\mathfrak{y}^{(l)}\cdot\mathbf{e}_2. \quad (6)$$

For the isotropic case the angular factors α^l are independent of l and so may be taken out of $\hat{\rho}_q$ and placed in front of Eq. (6). The operator $\hat{\rho}_q(t)$ is related in the usual way to $\hat{\rho}_q(0)$

$$\hat{\rho}_q(t)=e^{iHt}\hat{\rho}_q(0)e^{-iHt}. \quad (7)$$

Equation (3) for the cross section was arrived at by using the Golden rule to calculate the transition rate. The coupling to the electromagnetic field was treated in lowest order (i.e., Born approximation) and the initial state of the system was averaged over an equilibrium thermal ensemble. This approach is very similar to that used by D. G. although it differs from it in certain details. We present a more complete derivation of Eq. (3) in Appendix I.

In order to explicitly evaluate the cross section we must obtain an expression for the Fourier transform of the modified density-density retarded commutator.

$$F(\omega)=\int_0^\infty dt e^{i\omega t}\langle[\hat{\rho}_q(t),\hat{\rho}_{-q}(0)]\rangle. \quad (8)$$

The relation of the retarded commutator to an analytic continuation of the time-ordered temperature-dependent density-density propagator

$$G(u)\equiv\langle\{T\hat{\rho}_q(u)\hat{\rho}_{-q}(0)\}\rangle \quad (9)$$

is given in Ref. 9. The basic rules for the perturbation expansion of $G(u)$ and its diagrammatical representation are given in Ref. 10. To lowest order in e^2,[11] we find

$$G(\omega+i\epsilon)=\left[\alpha_i{}^2Q_i+\frac{\Phi Q_iQ_j\alpha_i\alpha_j}{\epsilon_T(q,\omega)}\right]V, \quad (10)$$

where

$$\Phi=4\pi e^2/q^2, \quad (11)$$

$$\epsilon_T=1-\sum_{i=1}^N\Phi_iQ_i. \quad (12)$$

V is the total volume of the system and

$$Q_i(q,\omega)=\int\frac{d^3p}{(2\pi)^3}\left[\frac{f_{p+q/2}{}^{(i)}-f_{p-q/2}{}^{(i)}}{\epsilon_{p+q/2}{}^{(i)}-\epsilon_{p-q/2}{}^{(i)}-\omega-i\epsilon}\right]. \quad (13)$$

The quantities $f_p{}^{(l)}$ are given by

$$f_p{}^{(l)}=[e^{\beta(\epsilon_p{}^{(l)}-\mu)}+1]^{-1}, \quad (14)$$

with

$$\epsilon_p{}^{(l)}=\mathbf{p}\cdot\mathfrak{y}^{(l)}\cdot\mathbf{p}/2m. \quad (15)$$

Equation (10) differs from what one would obtain for a set of spherical carriers only insofar as we have an effective inverse mass tensor $\mathfrak{y}^{(l)}$. Replacing $\mathfrak{y}^{(l)}$ by $\delta_{ij}\lambda^{(l)}$ will reduce Eq. (14) to the usual expressions for spherical carriers. The inverse mass tensor appears in Eq. (14) in two places, in the polarization factor, i.e., the unscreened response to an external field, and in the screening properties of the medium, i.e., into Q. Q_l for an ellipsoidal energy surface may be obtained from the well-known expressions [see Ref. 12, Eqs. (10)–(11)] where $\epsilon\equiv\epsilon_1+i\epsilon_2=1-(4\pi e^2/q^2)Q(q,\omega)$ for a spherical energy surface.

Call the matrix which diagonalizes the reciprocal

[9] A. Ron and N. Tzoar, Phys. Rev. **131**, 12 (1963).
[10] J. M. Luttinger and J. C. Ward, Phys. Rev. **118**, 1417 (1960).
[11] For the case of a degenerate semiconducting plasma the expansion is to lowest order in $(\hbar\omega_p/E_f)^2$. For a high-temperature nondegenerate plasma the expansion is $n_d{}^{-1}$, where n_d is the number of particles in a Debye sphere.
[12] A. J. Glick and R. A. Ferrell, Ann. Phys. (N. Y.) **11**, 359 (1960).

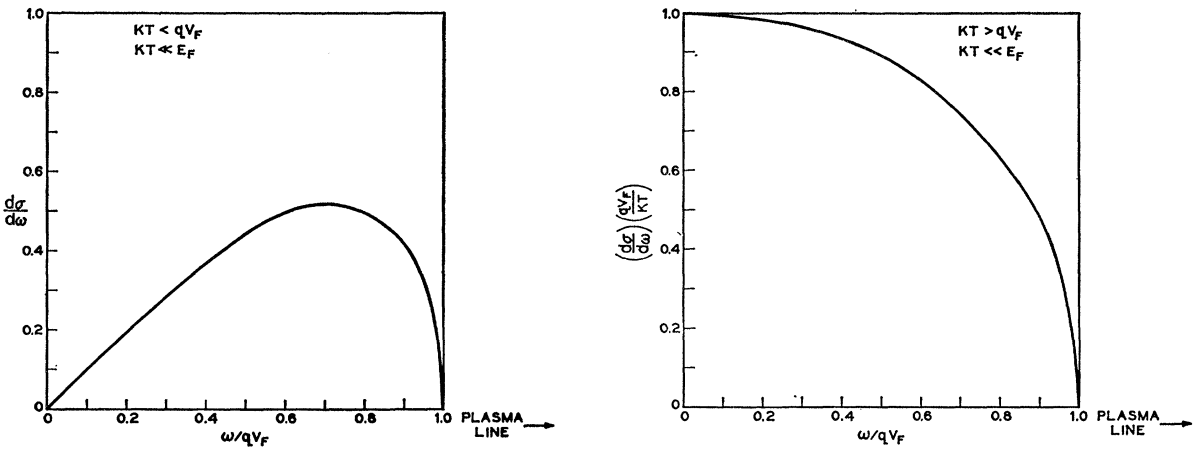

FIG. 2. Plot of the central line for scattering from a single degenerate isotropic carrier. The differential scattering cross section is normalized per unit volume per unit solid angle and the factor $r_0^2(qV_F/E_F)(q/q_{FT})^4$ has been divided out in (a) $kT<qV_F$ and in (b) $kT>qV_F$.

mass tensor Λ_{ij}, i.e.,

$$\mathbf{\Lambda}\cdot\mathfrak{y}\cdot\mathbf{\Lambda}^{-1}=\lambda_i\delta_{ij}, \tag{16}$$

where the quantities λ_i are the eigenvalues of the reciprocal mass tensor. It is then easy to show that

$$Q_e(\mathbf{q},\omega)=1/(\lambda_1\lambda_2\lambda_3)^{1/2}Q(S\mathbf{\Lambda}\cdot\mathbf{q},\omega). \tag{17}$$

S is a scaling operation, i.e., the vector $\mathbf{q}'\equiv\mathbf{\Lambda}\cdot\mathbf{q}$ has its components scaled with the eigenvalues of the effective mass tensor. More precisely, $\mathbf{q}''\equiv S\mathbf{\Lambda}\cdot\mathbf{q}$ is defined by components as

$$\begin{aligned} q_x''&=q_x'(\lambda_1)^{1/2}\\ q_y''&=q_y'(\lambda_2)^{1/2}\\ q_z''&=q_z'(\lambda_3)^{1/2}. \end{aligned} \tag{18}$$

We obtain an effective $\mathbf{q}$ vector by first rotating to principal axis and then scaling back to a sphere. The extra factor $1/(\lambda_1\lambda_2\lambda_3)^{1/2}$ is merely a volume factor which comes into a redefinition of the carrier density.

The final expression for the differential scattering cross section per unit volume is

$$\frac{d\sigma}{d\omega d\Omega}=-\frac{r_0^2}{\pi}\frac{1}{(1-e^{-\beta\omega})}\operatorname{Im}\left[\sum_{i=1}^{N}\alpha_i^2Q_i+\frac{\Phi Q_iQ_j\alpha_i\alpha_j}{\epsilon_T(q,\omega)}\right], \tag{19}$$

where Q_i is obtained from the spherical Q by a principal axis transformation and a scaling operation.

III. SINGLE CARRIER

For a single ellipsoidal carrier Eq. (19) reduces to

$$\frac{d\sigma}{d\omega d\Omega}=-\frac{r_0^2}{\pi}\frac{1}{(1-e^{-\beta\omega})}\alpha_1^2\frac{\operatorname{Im}Q_1(q,\omega)}{|1-\Phi Q_1(q,\omega)|^2}. \tag{20}$$

Here, the effect of the anisotropy is trivial. The over-all coefficient in front of Eq. (20) has been modified by an effective mass factor (an effective mass as determined by the incoming and outgoing polarization directions). The screening effect in the denominator has also been modified by a different effective mass factor (an effective mass as determined in this case by the direction of the momentum transferred in the scattering relative to the principal axis of the ellipse).

Let us examine Eq. (20) in more detail. In an analysis of the spectrum for a fixed q there are two frequency regions to consider.[13] In the low-frequency region where $\omega/qV_F<1$, the plasma statically screens any density fluctuations and the dielectric function is approximately given by

$$\epsilon_T\approx 1+q_{FT}^2/q^2, \tag{21}$$

where

$$q_{FT}^2=\omega_p^2/V_F^2. \tag{22}$$

The mass which comes into q_{FT} is the mass in the direction of the momentum transfer q. For $q<q_{FT}$ the central line is plotted in Fig. 2(a) for $kT\ll(qV_F)$. In this case the scattering cross section starts out proportional to ω and is of the order of a typical Thompson cross section times a screening factor $(q/q_{FT})^4$ and a factor (qV_F/E_F). The factor (qV_F/E_F) takes into account the degeneracy and the Fermi statistics. Crudely, it tells us the fraction of electrons which are participating in the scattering. The straight-line portion of the curve is simply related to the derivative of the one-dimensional Fermi distribution function $[f_0\sim 1-(V/V_F)^2]$. When $E_F\gg kT>qV_F$ the cross section in the central region is quite different [see Fig. 2(b)]. Under these conditions the cross section starts out independent of ω and is similar to the classical high-temperature central line except for its sharp cutoff at $\omega/qV_F=1$. [It is to be pointed out that quantities of

[13] In this discussion we assume that $q/2q_F\ll 1$.

order kT/E_F and qV_F/kT were neglected in the numerical evaluation of Fig. 2(b).] The classical central line is Gaussian in shape with a tail determined by kT.

In the high-frequency region with $\omega/qV_F \gg 1$ and $q \ll q_{FT}$,

$$\epsilon_T \approx 1-\omega_p^2/\omega^2. \tag{23}$$

It is well known[1,2,4] that there will be a resonance in the scattering cross section when $\omega=\omega_p$, the plasma resonance. In this approximation (lowest order in e^2) there is no width to the plasma line. The width will be produced by collisions with other species or with the lattice. The area under plasma line is to a good approximation independent of the exact collisional mechanism and of the order of,[14]

$$(d\sigma/d\Omega)_{\text{plasma}} \sim (q/q_{FT})^2 r_0^2. \tag{24}$$

IV. TWO ELLIPSOIDS

Now consider the case of two identical ellipsoids at right angles to one another (see Fig. 3). This model would be a reasonable one for describing the conduction band of silicon which has four equivalent ellipsoids in a plane. The pair of ellipsoids at opposite faces of the zone are identical while the pair on adjoining faces have their axes approximately rotated through ninety degrees. The two ellipses located in the plane at right angles to the one under consideration introduce no real complications into a calculation of the scattering cross section. For certain orientations of the scattering plane and specific choices of the incoming and outgoing polarizations of the light, these "extra ellipsoids" just produce a numerical factor in front of the total cross section. We will only consider the case of two ellipsoids as shown in Fig. 2.

In order to simplify the discussion, we discuss the central line ($\omega/qV_F \leq 1$) in the limit $q \to 0$ since this is where all the intensity is. To lowest order in q Eq. (19) may be written as

$$\frac{d\sigma}{d\omega d\Omega} = \frac{r_0^2(\alpha_1-\alpha_2)^2}{\pi(1-e^{-\beta\omega})} \operatorname{Im}\left(\frac{Q_1 Q_2}{Q_1+Q_2}\right). \tag{25}$$

We notice that in the neighborhood of the central line the cross section is of order $r_0^2(\alpha_1-\alpha_2)^2$ rather than of order $(q/q_{FT})^4 r_0^2$ as it was for the single-carrier case. The integrated area under the central line using Eq. (24) is easily shown to be of order

$$d\sigma_T/d\Omega \sim (\alpha_1-\alpha_2)^2 r_0^2. \tag{26}$$

If α_1 is equal to α_2, which obtains for certain definite polarization directions, it is necessary to go to higher order in q^2 in the expansion of the dielectric constant in Eq. (19). It is easy to show in this case that the central line has an area proportional to $(q/q_{FT})^4 r_0^2$. The quantities α_1 and α_2 are a direct measure of the response and subsequent reradiation of the charged carriers in the two ellipsoids.

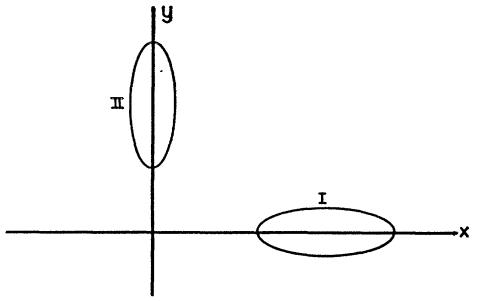

FIG. 3. Drawing of the Fermi surface for the carriers which are doing the incoherent scattering.

When the two α's are equal we have effectively a single carrier with somewhat modified screening properties and the area under the central line will be of the same order as for a single carrier, i.e., extremely small. When $\alpha_1 \neq \alpha_2$, we have in effect two carriers as for the electron-ion plasma in the nondegenerate case and there is a central line, whose area is of order 1.[15]

It is possible to have a resonance in the scattering due to the excitation of a sound-like mode in this "two-carrier" system. This resonance arises from a vanishing or near vanishing of the denominator in Eq. (25). Equation (25) may be rewritten to read

$$\frac{d\sigma}{d\omega d\Omega} = -\frac{r_0^2(\alpha_1-\alpha_2)^2}{\pi(1-e^{-\beta\omega})}\left[\frac{|Q_1|^2 \operatorname{Im}Q_2 + |Q_2|^2 \operatorname{Im}Q_1}{|Q_1+Q_2|^2}\right]. \tag{27}$$

Q_l in the limit $q/q_F \ll 1$ is

$$Q_l = -\tfrac{3}{4}(n/E_F)[ig(U^l)+h(U^l)], \tag{28}$$

where

$$g(U^{(l)}) = \pi U^{(l)} \theta(U^{(l)}-1) \tag{29}$$

and

$$h(U^l) = [U^{(l)} \ln|(U^l-1)/(U^l+1)|+2]. \tag{30}$$

$\theta(x)$ is the unit step function and

$$U^l = (\omega/q^l V_F). \tag{31}$$

The quantity V_F is defined by $\frac{1}{2}mV_F^2 = E_F$ and $q^{(l)}$ is the effective q relative to the axis of the ellisoid as defined (in general) in Eq. (18). For the special case under consideration, two ellipses at right angles (see Fig. 3), and a $\mathbf{q}$ in the x–y plane,

$$q^{(1)} = q[\lambda_1 \cos^2\theta + \lambda_2 \sin^2\theta]^{1/2}, \tag{32a}$$

$$q^{(2)} = q[\lambda_2 \cos^2\theta + \lambda_1 \sin^2\theta]^{1/2}. \tag{32b}$$

The angle θ is the angle the q vector makes in the x–y

[14] A. Ron, J. Dawson, and C. Oberman, Phys. Rev. **132**, 497 (1963).

[15] The fact that an anisotropic Fermi surface might give an enhanced central line scattering was first brought to the attention of the author by P. A. Wolff.

plane relative to the x axis. The mass tensor for the ellipse labeled as (1) in Fig. 2 is

$$\mu^{(1)}=\begin{bmatrix}\lambda_1 & 0 & 0\\ 0 & \lambda_2 & 0\\ 0 & 0 & \lambda_2\end{bmatrix}. \quad (33)$$

For $\lambda_2/\lambda_1>1$ it is possible to have the $\mathrm{Re}(Q_1+Q_2)=0$. In the extreme case of $\lambda_2\gg\lambda_1$, Q_2 is approximated by a constant (i.e., static screening). The value of $U^{(1)}$ which gives a root of $\mathrm{Re}(Q_1+Q_2)=0$ is determined from the equation

$$\delta(U^{(1)})\equiv -U^{(1)}\ln|(U^{(1)}-1)/(U^{(1)}+1)|=4. \quad (34)$$

The function $\delta(U^{(1)})$ is sketched in Fig. 4. There are two roots of Eq. (34), one for $U^{(1)}<1$ and one for

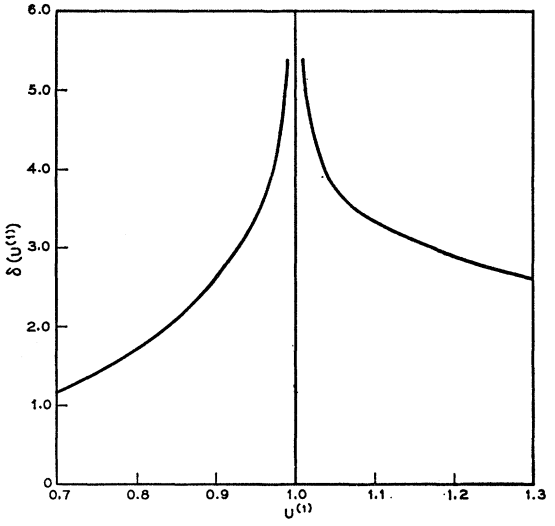

FIG. 4. Plot of the function $\delta(U^{(1)})$.

$U^{(1)}>1$. Both roots are sound-like, i.e.,

$$\omega/q\sim V_F{}^{(1)}. \quad (35)$$

The first root will not show up as a resonance in the scattering cross section since $\mathrm{Im}(Q_1+Q_2)$ is large for this root. For the root with $U^{(1)}>1$ the $\mathrm{Im}Q_1=0$, i.e., there is no damping of the mode due to the heavy carriers. The $\mathrm{Im}Q_2$ will be small since $\mathrm{Im}Q_2\sim U^{(2)}$ and $U^{(2)}\ll 1$, i.e., there is only a small amount of Landau damping due to the light carriers since the "mode" is traveling at a velocity which is much smaller than the Fermi velocity of the "light carrier." The behavior of the mode in this degenerate Q.M. case is quite different from the classical high-temperature case. For the classical case there is no sharp cutoff of the Landau damping due to the slow carriers, simply a gradual exponential decrease as the mode velocity becomes larger than the thermal velocity of the heavier carriers. Because of this the sound-like mode in the nondegenerate case is not well defined unless the temperature of the

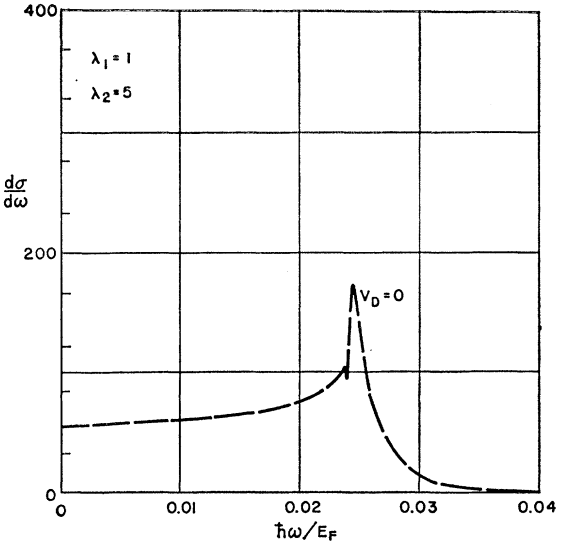

FIG. 5. Plot of the differential scattering cross section per unit volume per unit solid angle per particle normalized to the Thomson cross section r_0^2. The Fermi energy is fixed at 30 meV; there is no drift present and the two eigenvalues of the ellipsoidal mass tensor are 1 and 5.

light carriers is large compared to that of the heavy carriers.[16] The ratio of temperatures must be of order ten to one in order that there be a well-defined peak in the scattering cross section.[5]

Effect of Drifts

It is well known that small drifts in the plasma can produce large changes in the cross section in the neighborhood of the acoustic line.[5] An electric field

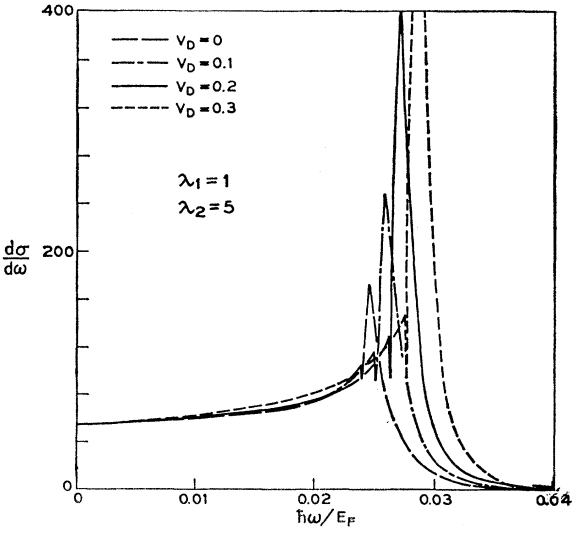

FIG. 6. The same plot as in Fig. 5 except that the drift velocity V_D of the heavy mass carrier is varied from curve to curve.

[16] B. D. Fried and R. W. Gould, Phys. Fluids 4, 139 (1961).

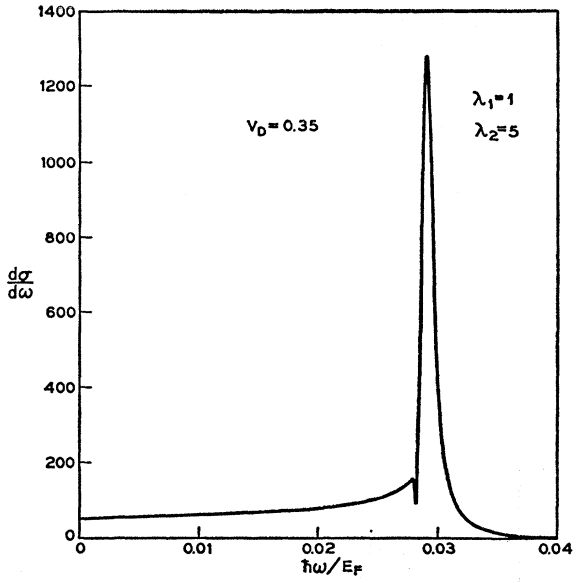

FIG. 7. Plot of the differential scattering cross section for a value of V_D near the instability.

applied to the plasma will drift the light carriers up to velocities which are of the order of the sound-mode velocities. The wave can then extract energy from these drifting carriers. Mathematically what happens is that the drift causes a shifting of the effective frequency ω which goes into the expression for Q_2. (The drift effect in Q_1 is smaller than in Q_2.) When

$$\omega - qV_{D2} = 0, \tag{36}$$

where V_{D2} is the "effective" drift velocity of the light carriers, then $\mathrm{Im}Q_2 = 0$ and the expression for the cross section diverges. As long as one considers only the lowest order terms in the expressions for Q_1 and Q_2, i.e., the simple bubble diagram, it is possible to show that the net effect of taking a drifted Fermi distribution for the carriers is to shift the frequency ω by $\mathbf{q}\cdot\mathbf{V}_{D1}$ or $\mathbf{q}\cdot\mathbf{V}_{D2}$, depending on which Q_e one is calculating. The statistical weighting factor $1/(1-e^{-\beta\omega})$ also has its frequency shifted by an amount which is determined by which $\mathrm{Im}Q_e$ it is multiplying in Eq. (27). The net effect of drift is to change the scattering cross section to

$$\frac{d\sigma}{d\omega d\Omega} = -\frac{r_0^2}{\pi}\left\{\frac{1}{[1-e^{-\beta(\omega-\mathbf{q}\cdot\mathbf{V}_{D1})}]}\frac{|Q_2|\,\mathrm{Im}Q_1}{|Q_1+Q_2|^2} + \frac{1}{[1-e^{-\beta(\omega-\mathbf{q}\cdot\mathbf{V}_{D2})}]}\frac{|Q_1|\,\mathrm{Im}Q_2}{|Q_1+Q_2|^2}\right\}, \tag{37}$$

where Q_1 and Q_2 are calculated using the appropriate shifted frequency. The simple modification is not correct to higher order in e^2, i.e., when one includes the effect of short-range collisions. The drifted distribution, with the two effective sets of carriers drifting at two different velocities is not an equilibrium situation. Collisions between the two sets of carriers will tend to destroy the nonequilibrium distribution.

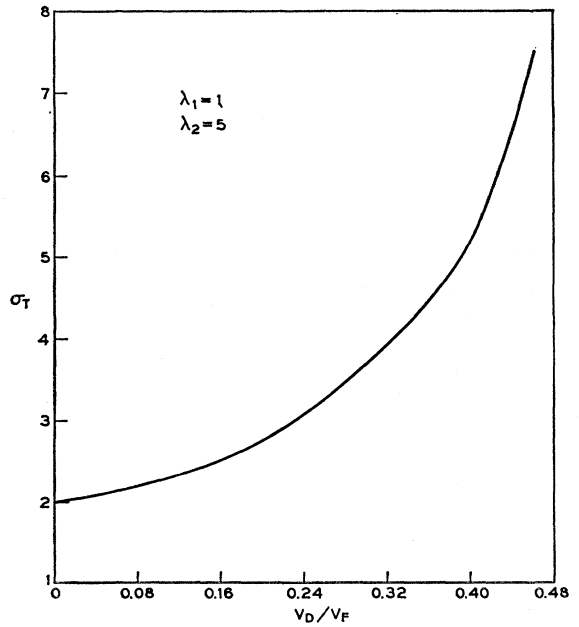

FIG. 8. Plot of total cross section as a function of V_D/V_F.

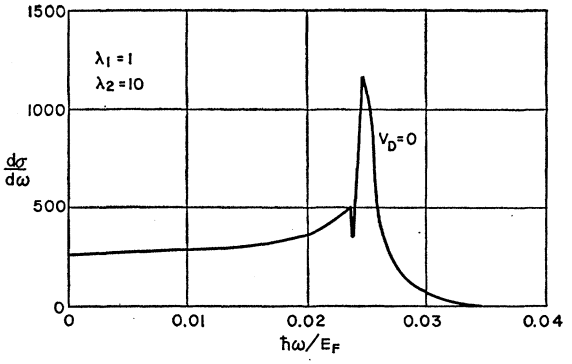

FIG. 9. The same plot as in Fig. 5 except for a change in the eigenvalues of the reciprocal mass tensor. The light mass direction is now 0.1 free-electron masses. The Fermi energy is 30 meV.

V. RESULTS OF NUMERICAL CALCULATIONS AND CONCLUSIONS

Consider the scattering to take place in the plane of the two ellipsoids. We will assume that the polarizations of the incoming and outgoing beams are also in the scattering plane (see Fig. 1). In Figs. 5–12, we have plotted the differential scattering cross section per particle per unit volume, per unit solid angle in units of r_0^2. The scattering cross section was evaluated for a fixed Fermi energy $E_F = 30$ meV, temperature $kT/E_F = 0.1$ scattering angle $\theta_s = \pi$ and $q/2q_F = 0.006$.

In evaluating these curves, the finite temperature was

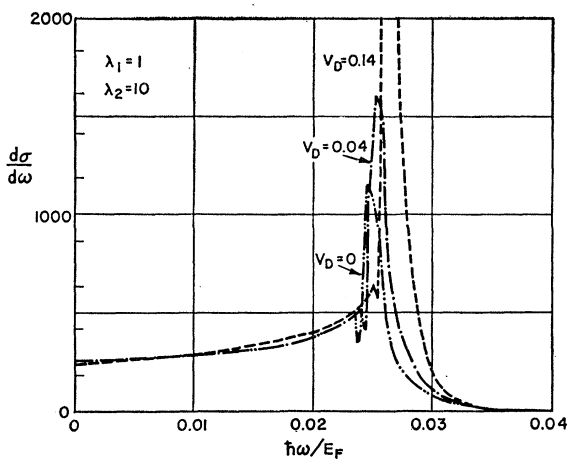

FIG. 10. Plot of the differential scattering cross section for a number of values of the drift velocity of the heavy carriers.

included in the statistical factor in front of the scattering cross section [see Eq. (37)]; however, it was not included in the evaluation of the Q_i. The temperature (kT) is small compared to E_F but is in fact large compared to $\hbar\omega$. This finite temperature, if it had been included in the evaluation of Q_i, would produce a smearing of all resonances which appear in Figs. 5–7 and 9–11 of order

$$(\Delta\omega/\omega)_{\text{temp.}} \simeq \tfrac{1}{2}(kT/E_F). \tag{38}$$

In addition, short-range collisions with impurities will produce an additional smearing which has not been included in the present analysis.

$$(\Delta\omega/\omega)_{\text{collisions}} \simeq (1/\omega\tau), \tag{39}$$

where τ is a phenomenological relaxation time. The net

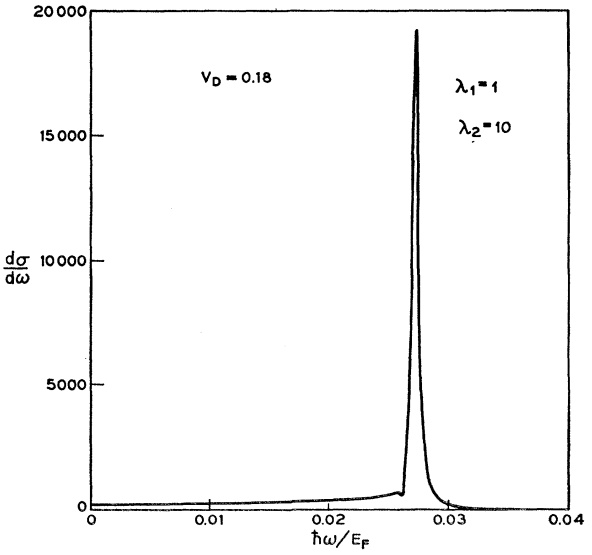

FIG. 11. Plot of the differential scattering cross section for a value of the drift velocity near the instability.

effect of these two mechanisms is a smearing of all resonances given approximately by

$$\Delta\omega/\omega \simeq \tfrac{1}{2}(kT/E_F) + (1/\omega\tau). \tag{40}$$

In Figs. 5 and 9 the drift velocity of the carriers has been set equal to zero. In Figs. 6–7 and 10–11, the drift velocity is varied from curve to curve. In Figs. 9 and 12, we have plotted the total cross section as a function of the drift velocity, where V_D is defined in terms of the applied dc electric field and the phenomenological collision time τ, i.e.,

$$V_D \equiv eE\tau/m. \tag{41}$$

In the first set of figures, Figs. 5–8, the mass anisotropy, i.e., the ratio of the long to short axis of the ellipse is

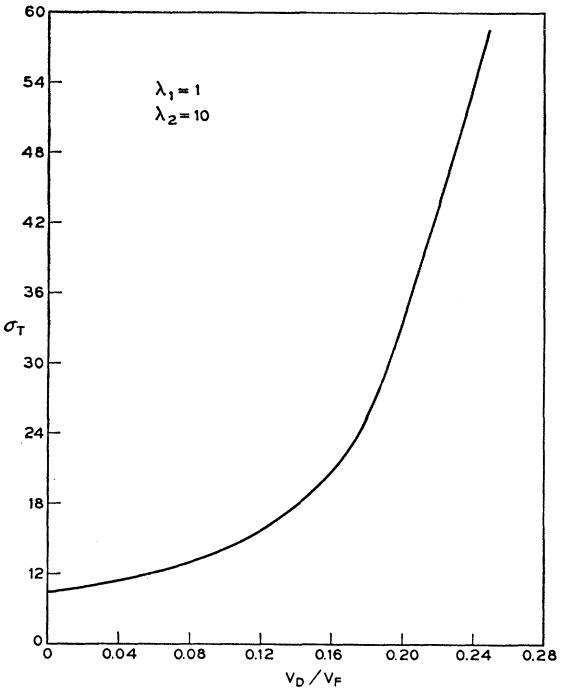

FIG. 12. Plot of the total cross section as a function of V_D/V_F.

taken to be five to one (the order of the mass anisotropy in silicon). In the second set of figures, Figs. 9–10, the mass anisotropy is taken to be ten to one(the order of the mass anisotropy in germanium).

All the plots of the differential scattering cross section show a well-defined peak at a value of $\omega/q \simeq V_F$ (of the heavy carriers). Approximately half the total area in the central line is in this peak. This peak is clearly due to the excitation of "plasma acoustic" modes. Even for the relatively small mass anisotropy of five to one which was used in Figs. 5–8 this acoustic peak is, unlike the nondegenerate case, well defined. The sharpness of the peak is a direct result of the sharp Fermi surface and to the discontinuous onset of Landau damping as discussed in Sec. IV. Increased mass anisotropy (Figs.

9–12) of ten to one sharpens up the peak. In addition, as the anisotropy is increased (if the heavy mass is held fixed) the total cross section goes up. This increase is simply due to the fact that the light mass carriers are doing most of the scattering so that the mass which comes into the Thompson cross section is small and the scattering increases.

Drift, even when it is as small as 0.01–0.05 of the Fermi velocity of the heavy carriers, produces significant changes in the peak cross section, in the position of the peak and in the total cross section. Of course, the larger the anisotropy the more effective the drift is since one is trying to drift the light carriers up to the velocity of the wave. With a ten to one mass anisotropy, a drift of $0.03V_F$, or approximately 3×10^5 cm/sec for a Fermi energy of 30 meV, produces a 20% change in peak cross section and a frequency shift of a few percent. Drift velocities of the order of a few times 10^5 may be reached experimentally. Electric fields producing drifts of that order could be used to modulate the inelastically scattered light intensity. Such a modulation scheme would be advantageous from an experimental point of view, in order to suppress unwanted background.

In all of the figures for the differential scattering cross section we note a sharp, extremely narrow, dip in the cross section in the neighborhood of the acoustic-mode resonance. It occurs at a frequency somewhat less than the acoustic-mode frequencies. The dip (which in our approximation will always be infinitely narrow) is due to the discontinuous behavior (see Fig. 3) of the function $\delta(U^{(1)})$ the Fermi velocity of the slow carrier. For a fixed $\mathbf{q}$ the position of the dip will determine the value of the Fermi velocity in the direction of $\mathbf{q}$.

The incoherent scattering of laser light from the electrons in the conduction band of a degenerate semiconductor can provide interesting information about the collective properties of the plasma and about the shape of the Fermi surface. The magnitudes of the cross sections are such that under suitable conditions an experiment is a definite possibility. Experimentally one should pick a semiconductor which has the following characteristics:

(a) It must be transparent to the laser light being used.

(b) It should have a relatively high mass anisotropy (the more the better). This anisotropy makes the acoustic mode well defined.

(c) It should have a light mass carrier (the lighter the better). The presence of a light mass carrier increases the total scattering cross section.

(d) The carriers should have a high mobility. A high mobility will allow one, by the use of external fields, to produce drifts in the carriers of the order of the phase velocity of the acoustic mode. This drift will enhance the cross section and furnish a means for modulating the signal.

ACKNOWLEDGMENTS

The author would like to thank P. A. Wolff, N. Tzoar, and S. J. Buchsbaum for many helpful discussions.

APPENDIX

In units in which $\hbar$ and c are equal to 1, the cross section per unit volume for the scattering of photons of wave vector and frequency k_1, ω_1, respectively, to photons of wave vector and frequency k_2 and ω_2 is

$$\frac{d\sigma}{d\omega d\Omega}=\left(\frac{\omega_2}{\omega_1}\right)r_0^2\bar{\sum_i}\sum_f|\langle f|\hat{\rho}_q|i\rangle|^2\delta(E_f-E_i+\hbar\omega), \quad \text{(A1)}$$

where $\hat{\rho}_q$ is defined in Eq. (5) of the text. The bar over the first summation sign indicates an average over an ensemble at a temperature $k_BT\equiv1/\beta$. The matrix element of $\hat{\rho}_q$ is taken between exact states of the many body system and $\omega\equiv|\omega_2-\omega_1|$. In arriving at Eq. (A1) the vector potential $\mathbf{A}$ of the E. M. field is normalized so that there is a unit probability per cubic centimeter of finding a photon, i.e.,

$$\mathbf{A}(x)=\sum_k\left(\frac{2\pi}{\omega}\right)^{1/2}[a_ke^{i\mathbf{k}\cdot\mathbf{x}}+a_k^\dagger e^{-i\mathbf{k}\cdot\mathbf{x}}]\mathbf{e}_k. \quad \text{(A2)}$$

Now write

$$\delta(E_f-E_i+\omega)=\frac{1}{(2\pi)}\int_{-\infty}^{+\infty}dte^{i(\omega+E_f-E_i)t}. \quad \text{(A3)}$$

Since

$$\langle f|\hat{\rho}_q|i\rangle e^{i(E_f-E_i)t}\equiv\langle f|\hat{\rho}_q(t)|i\rangle, \quad \text{(A4)}$$

it follows that (A1) may be written as

$$\frac{d\sigma}{d\omega d\Omega}=\frac{1}{(2\pi)}\left(\frac{\omega_2}{\omega_1}\right)r_0^2\int_{-\infty}^{+\infty}dte^{i\omega t}\langle\hat{\rho}_q(t)\hat{\rho}_{-q}(0)\rangle. \quad \text{(A5)}$$

We can now convert the correlation function to a commutator by noting that

$$\langle\hat{\rho}_{-q}(0)\hat{\rho}_q(t)\rangle=e^{-\beta\omega}\langle\hat{\rho}_q(t)\hat{\rho}_{-q}(0)\rangle, \quad \text{(A6)}$$

since

$$E_f-E_i=\omega.$$

Therefore,

$$\frac{d\sigma}{d\omega d\Omega}=\frac{1}{2\pi}\left(\frac{\omega_2}{\omega_1}\right)r_0^2\frac{1}{[1-e^{-\beta\omega}]}\int_0^\infty dte^{i\omega t}\times\langle[\hat{\rho}_q(t),\hat{\rho}_{-q}(0)]\rangle. \quad \text{(A7)}$$